Interaction Mechanisms between Poly(methyl Methacrylate) and Tricalcium Silicate (C₃S)

T. SUGAMA, L. E. KUKACKA, and W. HORN, *Process Sciences Division, Department of Energy and Environment, Brookhaven National Laboratory, Upton, New York 11973*

Synopsis

Interaction mechanisms between poly(methyl methacrylate) (PMMA) molecules and tricalcium silicate (C₃S) occurring in a C₃S-filled PMMA molecular structure before and after exposure to a simulated 25% geothermal brine solution at 240°C have been investigated by use of thermal analysis, infrared spectroscopy analysis, scanning electron microscopy, and compressive strength tests. For C₃S-filled PMMA samples before exposure to hot brine, it was observed that an interaction between the C₃S filler and the CH₂ groups in the main chain of the PMMA occurred. After exposure to the hydrothermal environment, indications were that the brine solution induced ionic bonding between the carboxylate anion (—COO⁻) groups in the PMMA and the Ca²⁺ ions from the C₃S. The reaction contributed to improvements in the thermal stability of the PMMA.

INTRODUCTION

Vinyl-type polymers having carboxylate groups in the molecules such as poly(methyl methacrylate) (PMMA) and trimethylolpropane trimethacrylate (TMPTMA) were evaluated to determine the feasibility of their use in concrete polymer composites for construction applications in geothermal processes. It was observed that when anhydrous cements containing calcium–silica compounds above ~70% were used as a filler with these polymers, significant improvement in the thermal stability of the composites occurred.[1] Depending upon the thermal environment (hot air or hydrothermal), the calcium–silica compounds appeared to affect the thermal stability in different ways. Therefore, it is possible that two different reaction mechanisms occur at the molecular interface between the PMMA layer and the calcium–silicate compound phase.

As reported in an earlier paper,[2] infrared analyses of PMMA–calcium–silica samples, before exposure to brine, indicated a reduction of the infrared peak absorbance of CH₂ groups in the region of 3020 to 2900 cm⁻¹. This was believed due to an interaction between the calcium–silica compound filler and the CH₂ groups in the main chains of vinyl-type polymers. In addition, it was interpreted that this interaction reduced the molecular mobility and flexibility of the CH₂ groups in the main chain, resulting in an increased thermal stability of the vinyl-type polymers.

The objective of the current study was to obtain detailed information regarding the two apparently different reaction mechanisms of PMMA with C₃S before and after exposure to hot brine. In order to obtain this information, thermogravimetric analysis (TGA), infrared (IR) spectroscopy, scanning electron microscopy (SEM) analysis, and compressive strength tests on C₃S-filled PMMA samples were performed. For purposes of comparison with the C₃S fillers, silica flour was also evaluated.

EXPERIMENTAL

Materials

Methyl methacrylate (MMA) monomer having a boiling point of 100° to 101°C, supplied by the Matheson, Coleman, and Bell Company as a laboratory sample, was used in this study. Polymerization was initiated by the addition of 2 wt % benzoyl peroxide of 98% purity and subsequent heating at 85°C for 24 hr.

C_3S containing a free lime concentration of 1.2% was synthesized in the laboratory by heating mixtures of pure calcium carbonate and silica gel at 1450°C. General commercial grade silica flour was used as a comparative filler material. Both the C_3S and the silica flour had a particle size of $<60 \mu$.

The composites were prepared by mixing 34 wt-% MMA with 66 wt % C_3S or silica flour. The materials were mixed thoroughly by hand for ~2 min. The mixture was then poured into 12-mm-diam. × 75-mm-long test tubes, covered with aluminum foil, and placed in an oven for curing at 85°C for 24 hr. Upon removal from the oven, the specimens were cooled and then ground to a size <0.104 mm.

The chemical constituents of the simulated 25% geothermal brine used in the autoclave in this study are shown in Table I.

Measurements

The thermogravimetric analysis measurements were performed using a du Pont Model 951 TGA at a heating rate of 10°C/min. Samples ranging in weight from 15 to 20 mg and crushed to a size <0.104 mm were used in the tests which were performed in nitrogen gas flowing at a rate of 80 ml/min.

The differential thermal analysis (DTA) measurements were conducted using a du Pont 910 differential thermal analyzer cell at a heating rate of 10°C/min in nitrogen gas. The DTA samples weighed 5 to 15 mg and were crushed to a size <0.104 mm.

A Perkin–Elmer Model 257 spectrometer was used for infrared analysis. The tests were performed by preparing KBr discs made by mixing 200 mg KBr and 3 to 5 mg of the sample that had been crushed to a size of <0.104 mm. The spectra were run at an 8-min scanning rate over the range of 4000 to 60 cm^{-1}.

Scanning electron microscopy observations were performed on the micro-

TABLE I
Chemical Constituents of 25% Brine Used in this Study

Chemical constituents	wt %
NaCl	11.77
KCl	2.75
CaCl	7.02
LiCl	0.11
$SrCl_2 \cdot 6H_2O$	0.12
$BaCl_2 \cdot 2H_2O$	0.04
$FeCl_3 \cdot 6H_2O$	0.85
$MnCl_2 \cdot 4H_2O$	0.43
$ZnCl_2$	0.09
Distilled Water	76.83

structured features of an interface structure between the PMMA and C$_3$S in the C$_3$S-filled PMMA samples. The samples were observed before and after exposure to brine and after an ethcing by immersion for 10 days in a 20% H$_2$SO$_4$ solution. The method of sample preparation for the SEM studies was to fracture a sample and, as soon as possible thereafter, deposit a gold film on the freshly fractured surface by evaporation and condensation.

Compressive strength tests were performed on duplicate samples before and after exposure to hot air and to a hot brine solution for 10 days at 240°C. Specimens 2.2 cm in diameter and 4.4 cm in length were used for compressive strength tests.

RESULTS AND DISCUSSION

Reaction Mechanism of PMMA with C$_3$S before Exposure to Brine

TGA Analysis. In order to investigate the degree of interaction between PMMA and C$_3$S and its dependance upon different curing temperatures, the weight loss of PMMA and of C$_3$S and silica flour-filled PMMA samples was measured from TGA curves. Samples prepared by three different curing conditions—24 hr at 85°C; 24 hr at 85°C and 24 hr at 100°C; and 24 hr at 85°C and 24 hr at 120°C—were tested. The results are presented in Table II.

These data indicate that the weight loss of bulk PMMA occurs rapidly near 200°C, probably because of the thermal decomposition of polymer. The weight losses occurring in the ranges 200° to 250°C and 250° to 300°C were about 7.2% and 26.8%, respectively. The weight loss of C$_3$S-filled PMMA samples which were cured at the same heating temperature as bulk PMMA showed a smaller weight decrease of 2.5% in the 200° to 250°C range when compared with that of bulk PMMA. However, in the range 250° to 300°C, the data indicate a weight decrease of 18.7%, which was assumed to be due to a gradual decrease in the effect of C$_3$S on the thermal stability of PMMA at temperatures above 250°C. The weight decrease of 3.5% at 200°C for silica flour-filled PMMA samples prepared by curing with the use of a two-step polymerization cycle for 24 hr at 85° and 120°C was greater than the 1.1% decrease obtained for C$_3$S-filled PMMA samples. This suggests that the addition of C$_3$S to PMMA improved the thermal stability of PMMA in the range of 100° to 250°C.

TABLE II
Weight Loss of Polymer for PMMA–C$_3$S or SiO$_2$ Systems

Composition	Curing temperature, °C	Weight loss,[a] wt %				
		150°C	200°C	250°C	300°C	350°C
100% PMMA	85 and 120	0.8	4.0	11.2	38.0	58.6
34% PMMA + 66% C$_3$S	85	0.4	3.6	8.0	28.4	48.0
	85 and 100	0.2	1.5	4.6	24.6	47.1
	85 and 120	0.1	1.1	3.6	22.3	46.6
34% PMMA + 66% SiO$_2$	85	0.8	4.8	10.8	29.7	52.4
	85 and 100	0.7	3.7	9.9	29.2	52.3
	85 and 120	0.7	3.5	8.6	28.9	48.9

[a] Average for two samples.

The results of TGA measurements for C_3S-filled PMMA samples also indicated that the weight loss in the temperature range of 100° to 300°C for samples prepared by using an additional cure period at 120°C was lower than that obtained by heating at 85° and 100°C. Samples containing silica flour did not exhibit this effect.

The fact that samples cured at the higher temperature had a lower weight loss in all cases may be due partially to less unreacted monomer and low molecular weight polymer in these samples. However, since the pure polymer sample, cured at 120°C, showed a substantially higher weight loss than filled samples cured at the same condition, this effect is considered to be unimportant.

On the basis of these observations, it appears that the degree of interaction at the interface between a PMMA layer and a C_3S grain becomes stronger with an increase in the curing temperature from 85° to 120°C.

IR Analysis. In a previous paper[2] the IR absorbance of CH_2 groups at 2940 cm^{-1} in PMMA–C_3S samples was shown to be much smaller than that for bulk PMMA, but at 1730 cm^{-1} the absorbance of $C{=}O$ groups was almost equal to that of bulk PMMA. Therefore, it was concluded that an interaction between the C_3S and the CH_2 groups in the main chains of vinyl-type polymers occurred.

In the current IR analysis, the relative reactivity between the CH_2 groups and the C_3S resulting from the two-step polymerization process was determined by calculating the absorbance ratio of the CH_2 groups at 2940 cm^{-1} and that of the $C{=}O$ groups at 1730 cm^{-1}. The absorbances were calculated by means of a base line method used in quantitative analysis, which measures the value and the distance from the absorption peak maximum to a baseline determined by connecting the two edges of the peak. The results of this analysis are presented in Table III.

The absorbance ratio of composites containing 34% MMA–66% C_3S and cured at 85° and 120°C decreases with an increase in the final heating temperature. This phenomenon is judged to be due to the distance between the interacting molecules of C_3S grains with CH_2 groups in the main chain of PMMA contracting with an increase in curing temperature, since the molecular mobility and flexibility of PMMA chain segments near the C_3S surface may be reduced by the strong interaction.

The results from TGA and IR analyses correspond to those recently reported[3-6]

TABLE III
Infrared Absorbance Analysis of PMMA Combined with C_3S or Silica Flour

Composition	Curing temperature °C	Absorbance ratio 2940 cm^{-1} CH_2/ 1730 cm^{-1} $C{=}O$[a]
100% MMA	85 and 120	0.74
34% MMA + 66% C_3S	85	0.24
	85 and 100	0.22
	85 and 120	0.17
3 MMA + 66% SiO_2	•85	0.52
	85 and 100	0.50
	85 and 120	0.68

[a] Average for two samples.

on the increase of glass transition temperature and improvement in the mechanical properties of glass beads, glass powder, mica flakes, and TiO_2-filled PMMA.

The data given in Table III also indicated that a prominent change in the absorbance ratio for silica flour-filled PMMA samples did not occur when the curing temperature was increased. This suggests that the main chain of PMMA is stronger than that for silica flour.

Reaction Mechanism of PMMA with C₃S after Exposure to Brine

IR Analysis. Results of the IR analysis are shown in Figures 1 to 3. In Figure 1, the IR spectra of anhydrous C_3S is characterized by a wide absorption band occurring around 840 cm⁻¹. IR absorption bands of C_3S-filled PMMA samples before exposure to brine, sample no. (b), indicate a symmetrical stretching vibration of CH_2 groups at 2940 cm⁻¹, a stretching vibration of C=O groups at 1710 cm⁻¹, and an asymmetric and symmetrical deformation vibration of the CH_3 groups at 1420 and 1130 cm⁻¹, a band which may be due to an asymmetric vibration of the C—O—C group.

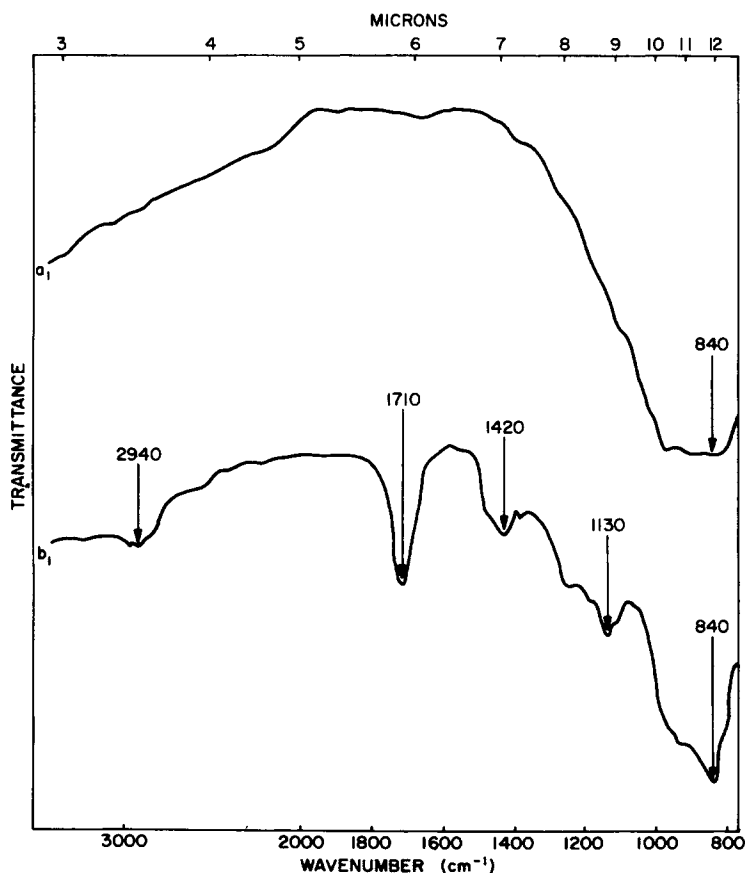In Figure 2, the spectrum for C_3S-filled PMMA samples after exposure for

Fig. 1. Infrared spectra of anhydrous C₃S and C₃S-filled PMMA: (a), anhydrous C₃S grains; (b) C₃S-filled PMMA before exposure to brine.
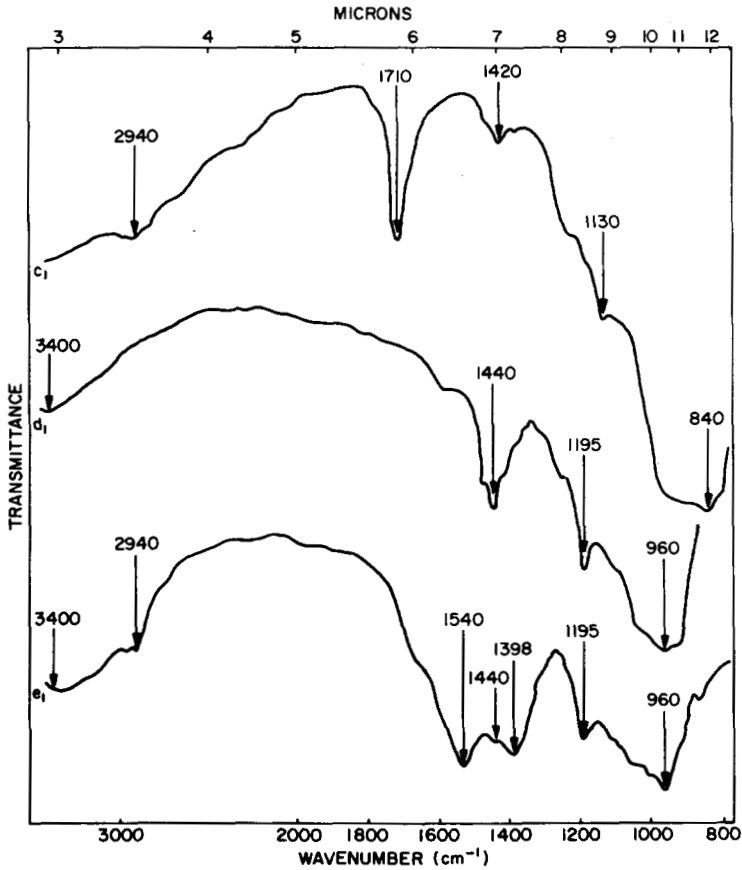
Fig. 2. Infrared spectra of hydrated C_3S and C_3S-filled PMMA after exposure to hot air and hot brine: (c), C_3S-filled PMMA after heating in a dry oven; (d), hydrated C_3S after exposure to hot brine; (e), C_3S-filled PMMA after exposure to hot brine.

10 days to hot air at 240°C, sample no. (c), was observed to be similar to that obtained from a control sample before exposure to hot air, sample no. (b) in Figure 1. This curve seems to demonstrate that an interaction of C_3S with PMMA molecules does not occur when the material is heated in a dry oven. The C_3S pastes were prepared with a water-to-C_3S ratio of 0.35 and subsequently cured under water for seven days at 25°C. The IR spectrum for the cured C_3S specimen after 10 days of exposure to brine at 240°C is represented by the curve identified as (d) in Figure 2. The spectrum has four major absorption bands due to the C_3S hydrate at 3400, 1440, 1195, and 960 cm^{-1}. This spectrum also indicates that the hydration products of C_3S can be recognized by the disappearance of the anhydrous C_3S band at 840 cm^{-1}.

The IR spectrum of C_3S-filled PMMA after exposure to brine, sample no. (e), illustrated a very interesting curve, namely, two new bands at 1540 and 1398 cm^{-1}. These bands represent asymmetric and symmetrical stretching vibrations of the COO^- (Ca) group, respectively, which may be due to ionic bonding occurring between Ca^{2+} ions and carboxylate anions (COO^-). It is believed that these bonds correspond to the results obtained from an IR study of the interaction between metal oxides and an aqueous solution of polyacrylic acid as reported by Leyte and Crisp et al.[7,8]
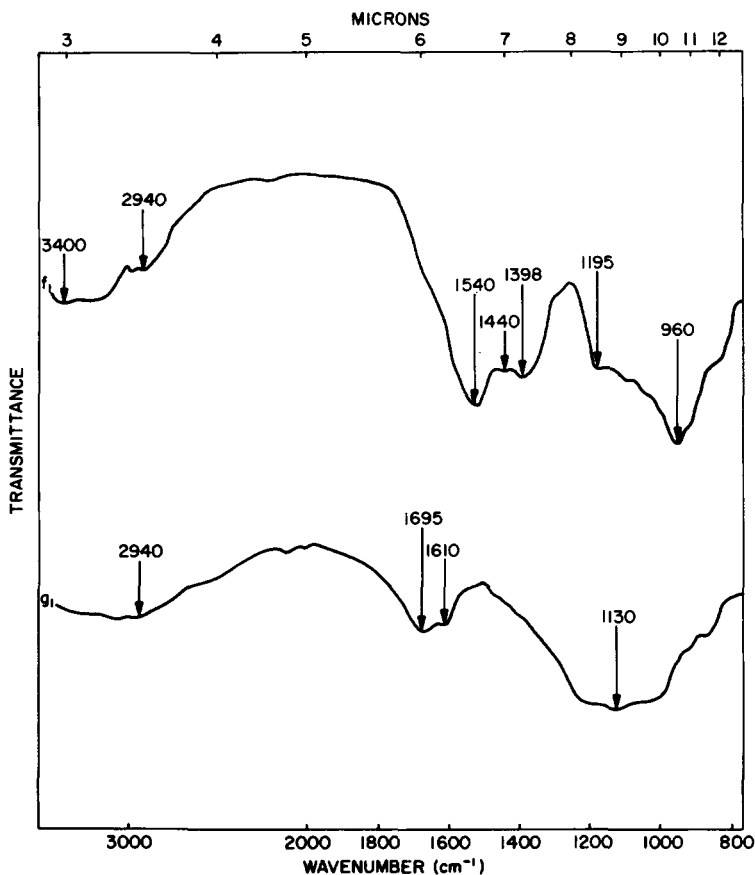
Fig. 3. Infrared spectra of C$_3$S-filled PMMA after immersing in benzene and 20% H$_2$SO$_4$: (f), C$_3$S-filled PMMA after immersion in benzene; (g), C$_3$S-filled PMMA after immersion in 20% H$_2$SO$_4$.

The chemical reaction mechanisms occurring at the interface of PMMA with C$_3$S grains are believed to be represented by a reaction process as shown in Figure 4. As indicated in the figure, Ca^{2+} ions are released readily by the attack of the hot brine on the anhydrous C$_3$S grains. Ca^{2+} ions produced in an aqueous medium develop an electrostatic interaction with the carboxyl groups (—C=O$^{\delta-}$) which become more strongly electropositive by the elevated temperature. Thus, the carboxylate group can be changed easily to the carboxylate anion (—COO$^-$) by the electrostatic interaction. The chemical effect of Ca^{2+} ions may be presumed to be a crosslinking function which connects two —COO$^-$ groups between PMMA chains and within a single chain.[9-11] A partial Ca–PMMA complex is covered with hydration products of C$_3$S which form under the conditions of high temperature and pressure in the autoclave.

The IR band reduction of CH$_2$ groups for C$_3$S-filled PMMA samples before exposure to brine was probably due to the restraining of segmented motion in amorphous polymer chains caused by the addition of C$_3$S to PMMA. Therefore, these Ca–PMMA complexes and hydration products of C$_3$S can be assumed to further restrain the moving segments of a linear polymer when exposed to an aqueous medium at an elevated temperature.
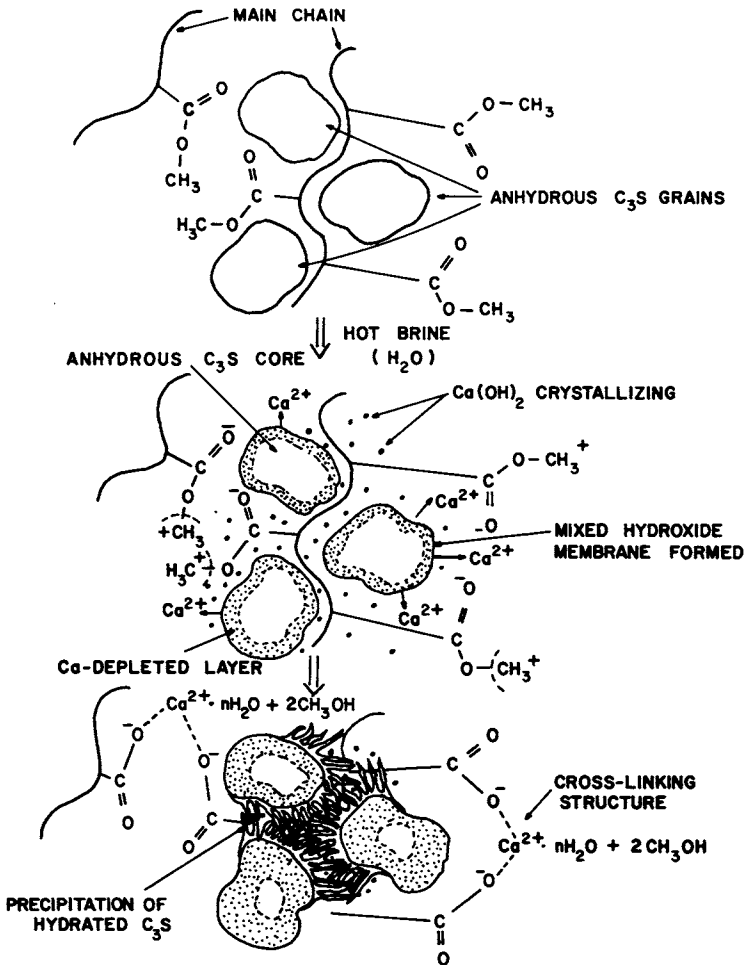
Fig. 4. Reaction mechanisms between C_3S and PMMA layer during exposure to brine.

The general configuration of polymer chains in an aqueous medium as described by Kuhn et al.[12] was represented by the following equation derived from a statistical consideration:

$$\overline{r^2} = ZAm^2 \tag{1}$$

where $\overline{r^2}$ = the average obtained by squaring the distance between the chain ends, Z = the number of segments per single chain polymer, and Am = the length of a segment. The total length (L_{max}) of a single chain is represented by $L_{max} = ZAm$.

Thus, eq. (2) indicates that the rate of coiling into a ball (Q) which occurs because of active segmental motion of polymer chains in a solution can be derived from eq. (1):

$$Q = \frac{L_{max}}{(\overline{r^2})^{1/2}} = Z^{1/2} \tag{2}$$

This equation states that the rate of polymer coiling lowers with a lengthening of the distance between chain ends.

It is very interesting to consider with reference to eq. (2) how the Ca^{2+} ions can restrain a molecular coil of polymer chains caused by hydrothermal conditions. A crosslinking mechanism caused by Ca^{2+} ions connecting two —COO⁻ anions may take place in two forms, namely, between PMMA chains and within a single chain.

For the crosslinking function of Ca^{2+} which connects two different polymer chains, a relative extension of the distance between the two single chains caused by the ionic bonding of Ca^{2+} ions with two —COO⁻ anions may increase the value of $\overline{r^2}$ in eq. (2), and this effect may restrain the polymer chains from coiling into a ball.

For the restraining of segmented motion due to the ionic bonding of the Ca^{2+} ions with two carboxylate anions within a single polymer chain, the Ca^{2+}, having a large radius of about 0.99 Å,[13] may increase the distance between two —COO⁻ anions. It can be assumed that this bonding also may help to keep the chain straighter and prevent it from balling up.

Also, it is possible that the hydration products of C_3S have a sufficient restrictive effect against the moving segments of linear polymer which occur in an aqueous medium at high temperature.

The IR spectra of Ca–PMMA complex samples after exposure for 10 days to a benzene solvent and 20% H_2SO_4 at 40°C are presented in Figure 3. From the results for sample no. (f) given in the figure and by comparison with results before exposure to benzene, it appears that the chemical stability of Ca–PMMA complex in the solvent is excellent. However, the spectrum of the sample exposed to H_2SO_4, sample no. (g), was considerably different from the one before exposure to the acid. The most significant change in the spectrum is the occurrence of
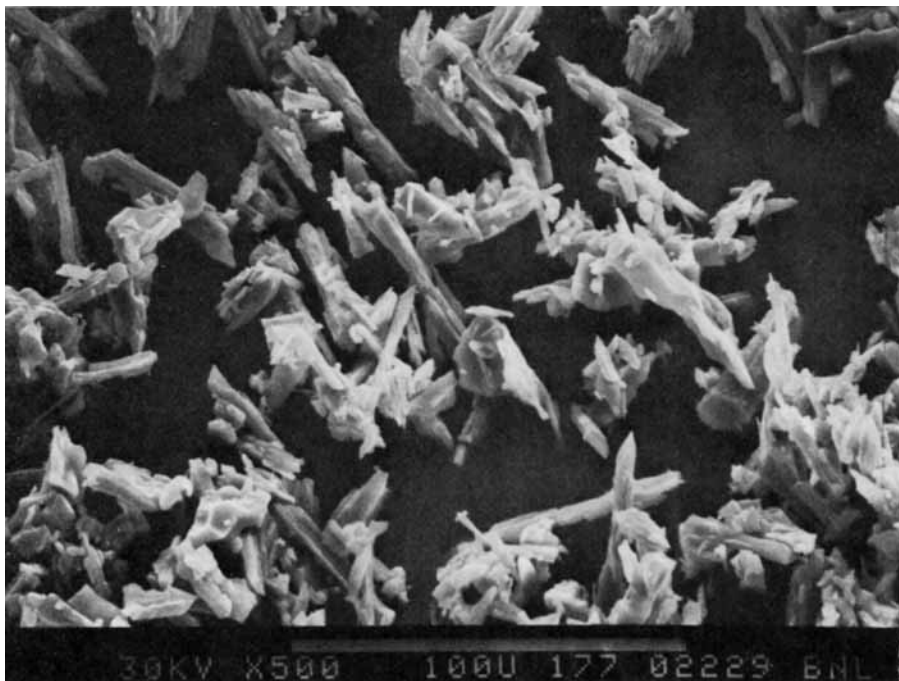

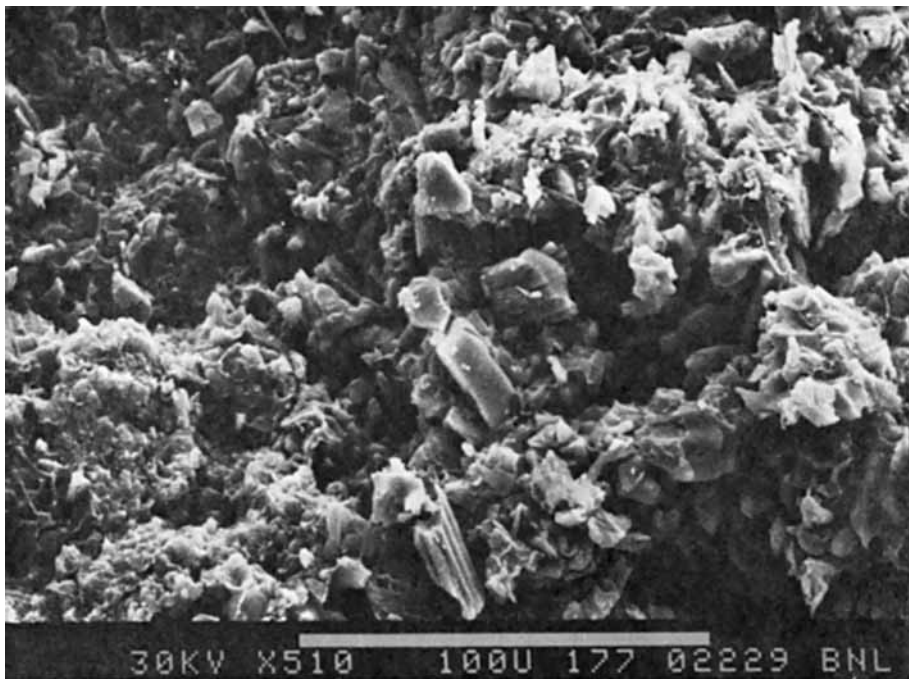Fig. 5. Scanning electron micrograph of anhydrous C_3S grains.

Fig. 6. Scanning electron micrograph of the fracture surface of C_3S-filled PMMA before exposure to brine.

three new peaks at 1695, 1610, and 1130 cm^{-1} in place of the peaks which represented the hydration products of C_3S. The spectra also suggest that all of the hydration products and a partial amount of the Ca–PMMA complex are destroyed by the attack of the highly concentrated H_2SO_4 solution. The absorption band at 1695 cm^{-1} may be due to the carboxylic acid (COOH) group produced by the exchange reaction of Ca^{2+} ions in the Ca–PMMA complex with H^+ ions from the H_2SO_4 solution. The weak peak at 1610 cm^{-1} is associated with the residual ionic bonding of Ca^{2+} ions and $-COO^-$ anions. A strong absorption peak around 1130 cm^{-1} may be due to sulfur tetroxide ions (SO_4^{2-}) which are derived from the exchange reaction between the Ca–PMMA complex and the H_2SO_4 solution.

SEM Study. In order to observe the microstructural features of C_3S-filled PMMA samples before and after exposure to hydrothermal conditions, scanning electron microscopy studies were performed. Scanning electron micrographs of the fractured surfaces of anhydrous C_3S grains, hydrated C_3S, and C_3S-filled PMMA samples before and after exposure to hot brine are shown in Figures 5 to 8. In addition, the fracture surface of etched C_3S-filled PMMA samples after exposure to brine and subsequent immersion for 10 days in 20% H_2SO_4 are also presented in Figure 9.

Figure 5 shows the anhydrous C_3S grains having sharply pointed shapes. The fracture surface of samples prepared by mixing MMA monomer with C_3S is illustrated in Figure 6. The microscopic structure of PMMA in the C_3S-filled PMMA sample was observed to have a continuous layer connecting C_3S grains. A typical micrograph of the fracture surface of hydrated C_3S prepared by im-

Fig. 7. Scanning electron micrograph of the fracture surface of hydrated C$_3$S with a water to C$_3$S ratio of 0.35 cured in an autoclave for 10 days.

mersion in an autoclave for 10 days at 240°C is shown in Figure 7. The fiber-like structures are crystals of hydrated C$_3$S and this structure forms the spiny network.

In the micrograph of C$_3$S-filled PMMA samples after exposure to hot brine, the Ca–PMMA complex layers were observed to be completely covered by the spiny network structure of hydrated C$_3$S crystals, Figure 8. Also, it can be seen from the micrograph that the hydrated C$_3$S crystals grow from the Ca–PMMA complex as if from an arable land.

Figure 9 indicates that all of the hydrated C$_3$S crystals were removed from the Ca–PMMA complex structure by the attack of the H$_2$SO$_4$ solution, and this microstructure seems to represent a three-dimensional polymeric structure.

Thermal Behavior Analysis. The thermal stability of the Ca–PMMA complex produced by the ionic bonding of Ca^{2+} ions with carboxylate (COO$^-$) ions was investigated by TGA and DTA analysis. As shown in Figure 10, the TGA curve of the Ca–PMMA complex indicates that the weight loss of material begins to occur slowly at approximately 300°C, exclusive of the weight decrease occurring rapidly in a range of about 40° to 150°C, which is probably due to vaporization of neutral H$_2$O molecules coordinated to Ca^{2+} ions in Ca^{2+} bridges.[14] The temperature at which approximately 25% weight loss of the complex occurs is about 570°C. Compared to the onset temperature of thermal decomposition obtained from the TGA curve of the Ca–PMMA complex, the thermal decomposition of C$_3$S-filled PMMA samples before exposure to brine occurs gradually at around 200°C which is a temperature lower by about 100°C. This curve also indicates that the 25% weight loss of product takes place at about 390°C.

Fig. 8. Scanning electron micrograph of the fracture surface of C_3S-filled PMMA after exposure to brine.

From the DTA thermogram of the Ca–PMMA complex, it is observed that a large exothermal peak occurs at about 480°C at the same time that the thermal degradation of the unexposed complex nears completion. The broad exothermal peak at about 80°C is probably a result of the influence of neutral H_2O molecules coordinated to those Ca^{2+} ions in Ca^{2+} bridges, as described in the TGA curve. On the contrary, the thermogram of C_3S-filled PMMA before exposure to brine is characterized by two large exothermal peaks at about 320° and 390°C, and the peak at 390°C seems to represent the end temperature of degradation of PMMA itself.

In order to determine the thermal stability of the Ca–PMMA complex at 200°, 300°, and 350°C, tests were performed using a du Pont TGA operated in the isothermal mode. The results, given in Figure 11, indicate good thermal stability at 300°C after an initial rapid loss of weight, probably due to the neutral coordinated H_2O molecules. The curve for the complex at 350°C indicates a gradual weight loss with time. This indicates the limit of its thermal stability. The curves of C_3S-filled PMMA before exposure to brine indicate a good thermal stability at 200°C. However, at 300° and 350°C, there is a rapid degradation of PMMA with time.

From the results of the thermal behavior tests described above, it appears that the thermal stability of the Ca–PMMA complex produced by ionic bonding between the Ca^{2+} cations and the polyanions in a hot brine medium is far better than that of C_3S-filled PMMA before exposure to brine.

Compressive Strength. The physical properties of the Ca–PMMA complex were investigated by compressive strength tests of polymer mortar prepared by
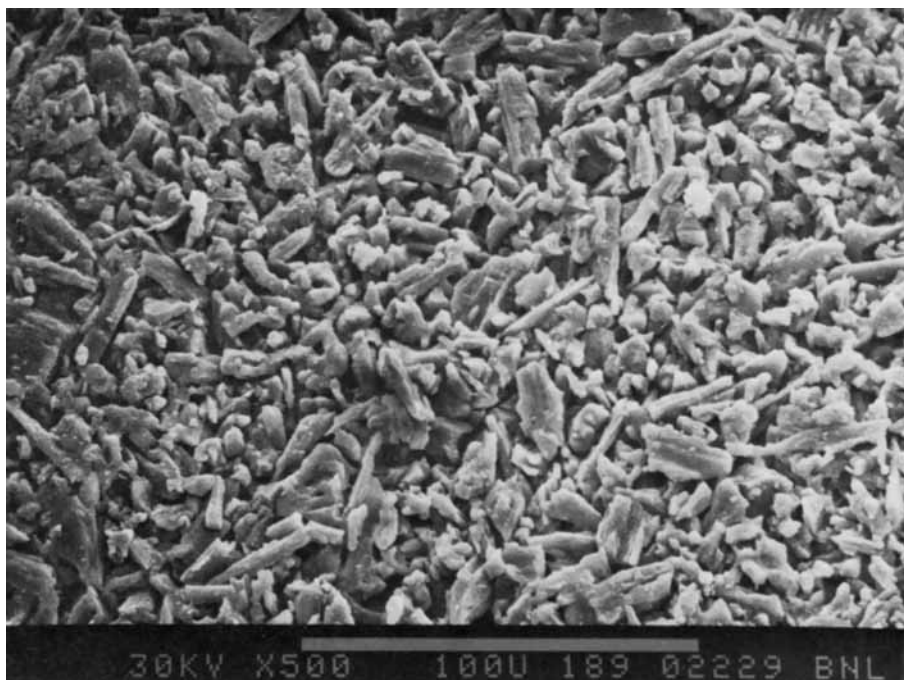
Fig. 9. Scanning electron micrograph of the fracture surface of Ca-PMMA complex after etching with 20% H$_2$SO$_4$.

the addition of 70 wt % silica sand to 12 wt % MMA monomer containing 18 wt % C$_3$S. Silica flour was also evaluated as a filler for polymer mortar in this study, and comparison was made with C$_3$S results.

The results given in Table IV indicate that the strength of Ca–PMMA complex polymer mortar formed during the brine exposure is 54.2 MPa. However, the silica flour-filled PMMA polymer mortar specimens failed in the test as a result of the large expansion produced by the thermal decomposition of the polymer.

The strength reductions of PMMA polymer mortar containing 18% C$_3$S after 10 days in brine and in a dry oven at 240°C were ~56% and 84%, respectively. It appears from these results that the Ca–PMMA complex in polymer mortar formed by the hydrothermal conditions has a far more significant effect on the thermal stability of PMMA polymer mortars than the effect of only the interaction which occurs between the C$_3$S grains and the CH$_2$ groups. Also, the hydration products of C$_3$S which are formed in the hydrothermal environment contribute significantly to the improved compressive strength of samples after exposure to brine.[15] Furthermore, the data suggest that the addition of only 18% C$_3$S to polymer mortar makes it possible to significantly improve the thermal stability of PMMA polymer mortar to 240°C.

CONCLUSIONS

From the data presented and the discussion just given, some definite conclusions are possible. The interaction occurring between the C$_3$S grains and CH$_2$ groups within the main chain of the PMMA molecule appears to have a reductive
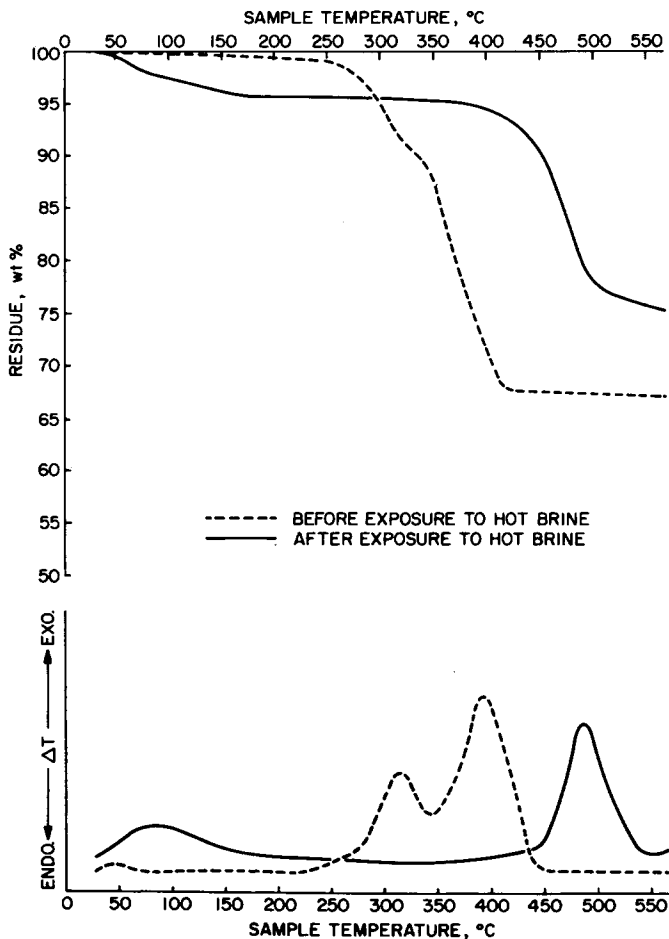
Fig. 10. TGA and DTA thermograms of C_3S-filled PMMA before (- - -) and after(—) exposure to 25% brine at 240°C.

TABLE IV
Compressive Strength of PMMA Polymer Mortar Containing C_3S or Silica Flour

	Compressive strength,[b] psi (MPa)		
Composition[a]	Before exposure	After exposure to hot air at 240°C for 10 days	After exposure to brine at 240°C for 10 days
12% P–70% S–18% SiO_2	11,480 (79.1)	371 (2.6)	—[c]
12% P–70% S–18% C_3S	17,530 (120.8)	2,850 (19.6)	7,735 (53.3)

[a] P = MMA; S = 50 wt% #16 sand (size 1.19 mm)—25 wt-% #30 sand (size 0.595 mm)—25 wt % #100 sand (size 0.149 mm); SiO_2 = silica flour; C_3S = tricalcium silicate.

[b] Values are averages for two 2.2-cm-diam × 4.4-cm-long cylinder specimens.

[c] Failed (large expansion) and removed from test.

effect on the molecular mobility and flexibility of the PMMA chain segments. This significant effect has a considerable influence on the thermal stability of the PMMA near 200°C as shown by the TGA and DTA curves. The addition of C_3S to PMMA having carboxylate groups in the molecule results in ionic
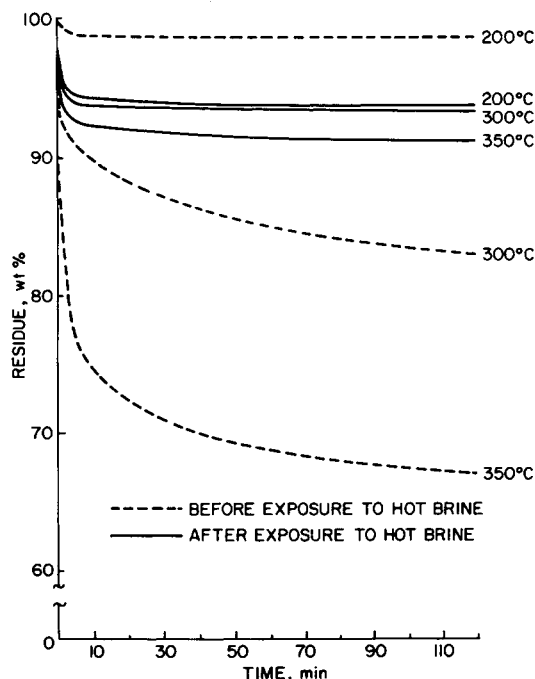
Fig. 11. Isothermal degradation of the MMA-C3S system before (- - -) and after (—) autoclave exposure.

bonding between Ca^{2+} ions of the C_3S and COO^- anions of the PMMA during exposure to hot brine at 240°C. The Ca–PMMA complex thus formed may prevent the thermal decomposition of the polymer itself caused by the cross-linking function of Ca^{2+} which connects two COO^- ions.

References

1. L. E. Kukacka, J. Fontana, W. Horn, J. Amaro, and T. Sugama, Alternate Materials of Construction for Geothermal Applications, Progress Report No. 11, October–December 1976, BNL 50627 New York.

2. T. Sugama and L. E. Kukacka, *J. Cement Concrete Res.*, **9**, 69 (1979).

3. I. Galperin, *J. Appl. Polym. Sci.*, **11**, 1475 (1967).

4. YU. S. Lipatov and F. Y. Fabulyak, *J. Appl. Polym. Sci.*, **16**, 2131 (1972).

5. K. Iisaka and K. Shibayama, *J. Appl. Polym. Sci.*, **22**, 1321 (1978).

6. K. Iisaka and K. Shibayama, *J. Appl. Polym. Sci.*, **22**, 3135 (1978).

7. J. C. Leyte, L. H. Zuiderweg, and H. J. Vledder, *Spectrochim. Acta*, **23A**, 1397 (1967).

8. S. Crisp, H. J. Prosser, and A. D. Wilson, *J. Mater. Sci.*, **11**, 36 (1976).

9. F. T. Wall and S. J. Gill, *J. Phys. Chem.*, **58**, 1128 (1954).

10. I. Michaeli, *J. Polym. Sci.*, **48**, 291 (1960).

11. A. D. Wilson and S. Crisp, *Organolithic Macromolecular Materials*, Applied Science Publishers, London, 1977, p. 126.

12. W. Kuhn and H. Kuhn, *Helv. Chim. Acta*, **26**, 1394 (1943).

13. R. C. Weast, *Handbook of Chemistry and Physics*, 49th ed., Chemical Rubber, Cleveland, OH, 1968, p. F-152.

14. A. D. Wilson and S. Crisp, *Br. Polym. J.*, **6**, 165 (1974).

15. T. Sugama, L. E. Kukacka, and W. Horn, *J. Cement Concrete Res.*, 9(4), 461 (1979).